# New splitting formulations for lattice summations

Paul F. Batcho[a] and Tamar Schlick[b]
*Department of Chemistry and Courant Institute of Mathematical Sciences, New York University, New York, New York 10012 and The Howard Hughes Medical Institute, New York, New York 10012*

(Received 23 March 2001; accepted 27 August 2001)

We present a new formulation for the efficient evaluation of pairwise interactions for large nonperiodic or spatially periodic infinite lattices. Our optimally designed splitting formulation generalizes the Ewald method and its Gaussian core function. In particular, we show that a polynomial multiplication to the Gaussian core function can be used to formulate desired mathematical or physical characteristics into a lattice summation method. Two optimization statements are examined. The first incorporates a pairwise interaction splitting into the lattice sum, where the direct (real) and reciprocal space terms also isolate the near-field and far-field pairwise particle interactions, respectively. The second optimization defines a splitting with a rapidly convergent reciprocal space term that allows enhanced decay rates in the real-space term relative to the traditional Ewald method. These approaches require modest adaptation to the Ewald formulation and are expected to enhance performance of particle-mesh methods for large-scale systems. A motivation for future applications is large-scale biomolecular dynamics simulations using particle-mesh Ewald methods and multiple time step integration. © *2001 American Institute of Physics.* [DOI: 10.1063/1.1412247]

## I. INTRODUCTION

The evaluation of a sum of point Coulomb charges and higher-order dispersion lattices is fundamental to many fields of chemical physics. For electronic structure calculation of a crystalline lattice, such a summation is required over all nuclei for the nuclear-electron repulsion term.[1] Likewise, evaluation of the electrostatic potential for large material science and biomolecular dynamics simulations has its most significant computational bottleneck at the evaluation of the Coulomb lattice sum.[2] Coulomb and lattice applications also abound in crystallography and in fields such as hydrodynamics and astrophysics.

There has been a rich history on the efficient calculation of the direct lattice sum;[3–7] see Ref. 8 for a recent review on biophysics applications. The underlying problems are the slow, conditional convergence of the direct summation of a large or infinite crystal lattice and the associated $N^2$ work.

Possibly the most successful method for reformulating the Coulomb lattice sum was first proposed by Ewald,[7] who split the sum into a rapidly convergent sublattice sum and a second potential that requires a solution of Poisson's equation. At first glance, the replacement of a sum by a solution of a partial differential equation in three dimensions would seem to be questionable. However, Ewald's use of a Gaussian core function results in a highly favorable reciprocal-space decay in the Poisson kernel for a periodic lattice, and equally satisfactory decay of the real-space component. The combined effect is a mathematically consistent formulation that is well suited for computational methods.

The basic Ewald formulation has largely remained unchanged for nearly 80 years. However, new applications in fields such as molecular dynamics, condensed matter physics, and material science impose increasing demands on the efficient use of computational formulations and mathematical constructions. Several studies have extended the Ewald formulation to higher-order dispersion effects[9–13] through the incomplete gamma function, and recently to the splitting of the Yukawa potential.[14] Studies of alternative non-Gaussian core functions have been presented in Refs. 5 and 15; however, the Ewald Gaussian function remains the standard for lattice sum formulations.

For a practical computational implementation to large crystal unit cells, a particle-mesh approach is typically adapted to Ewald's method.[6,13,16–19] The three basic particle-mesh computational formulations, namely particle–particle–particle mesh ($P^3M$), particle-mesh Ewald (PME), and smooth PME, have recently been re-examined by Deserno *et al.*[19] From a different perspective, formulations that split large lattice sums into far-field and near-field terms via the multipole expansion have been proposed in the fast-multipole framework (FMM);[20,21] however, recent evidence[22,23] indicates that the PME method has an advantage in computational cost over FMM methods for molecular dynamics simulations over 20 000 particles. An application of the FMM method to the real-space sum of the Ewald method has also been implemented.[24]

Our goal is to build upon the success of Ewald's Gaussian formulation and expand its favorable properties to create new splitting methods that are advantageous in certain applications and offer similar, if not better, convergence. Namely, we examine the incorporation of new properties, such as including a physical-space pairwise-interaction splitting into

[a]Electronic mail: paul@biomath.nyu.edu; fax: 212-995-4152.
[b]Electronic mail: schlick@nyu.edu

 

the real/reciprocal-space splitting. We also show that a high-degree polynomial multiplied by the Ewald Gaussian core function can be optimally designed to result in a more efficient lattice sum. In the adaptation of the Ewald method to higher order dispersion terms,[12] polynomial/Gaussian core functions have been used; here we generalize the Ewald formulation by using several different functionals.

Systematic construction of core functions, their Fourier transforms, and switch functions for the real space sum are presented. First, the splitting of the lattice sum is studied where the real space sublattice is designed to isolate near-field particle interactions. This splitting characteristic is not found in the Ewald formulation; it is a disadvantage in biomolecular simulations, limiting computational speedups when multiple-time-step (MTS) integration is used.[25,26] Thus, a modification that addresses this weakness is expected to offer advantages in the implementation of PME/MTS approaches. Second, we formulate an optimization problem to design a core function with a more rapid rate of decay in the reciprocal space while maintaining an equivalent, or better, rate of decay for the real-space sum (compared to Ewald's Gaussian function). We examine properties of optimal core functions and suggest several new avenues to optimally design an efficient lattice sum to meet desired properties.

In Sec. II we present a formulation of the Ewald-type splitting of the Coulomb potential and establish its relevance to the lattice sum and our optimization statements. Section III proposes general core functions and presents the necessary integral evaluations for constructing their Fourier transforms and switch functions for the real-space sum. Section IV introduces the optimization statements for the pairwise-interaction splitting and reciprocal-space decay rate. Preliminary results are also presented, along with the mathematical constructions. Specifically, Sec. IV A addresses the pairwise interaction splitting and Sec. IV B extends the pairwise interaction splitting to a multilevel splitting to account for more than two force components. In Sec. IV C, we present an analysis that allows for a construction of a core function that has an optimized rate of convergence in reciprocal-space and contrast the results to the traditional Ewald method. Three appendices provide the technical details that allow a systematic construction of the core functions and their transforms. Section V summarizes the formulations and results.

## II. SPLITTING FORMULATION

We consider a neutral system of $N$ point charges $q_1,q_2,\ldots,q_N$, at positions $\mathbf{r}_1,\mathbf{r}_2,\ldots,\mathbf{r}_N$, in a unit cell. The electrostatic energy of the system is defined by the interaction of each point charge with all the other point charges in the infinite periodic lattice,

$$\frac{1}{2}\sum_{i,j=1}^{N} q_i q_j {\sum_{|\mathbf{n}|}}' \frac{1}{|\mathbf{r}_{ij}+\mathbf{n}|}. \tag{1}$$

Here $\mathbf{r}_{ij}$ is the particle–particle separation, and the prime symbol in the summation ($\Sigma'_{|\mathbf{n}|}$) indicates that for $|\mathbf{n}|=0$ we omit the $i=j$ interaction. The Ewald sum relies on a consistent mathematical splitting of the sum into a near-field sum and a global solution of a partial differential equation.

Our presentation here of the Ewald sum formulation is appropriate for our proposed developments. We start with the splitting of the Coulomb potential in three dimensions, $G(\mathbf{r}-\mathbf{r}')=1/|\mathbf{r}-\mathbf{r}'|$, where $\mathbf{r}-\mathbf{r}'$ is an interpair distance vector and $G(\mathbf{r}-\mathbf{r}')$ is the Green's function associated with Poisson's equation, by introducing a particle core function, $\sigma(\mathbf{r}-\mathbf{r}')$, and a new multi-centered charge distribution $\rho(\mathbf{r})$,

$$\rho(\mathbf{r})=\sum_j q_j \sigma(\mathbf{r}-\mathbf{r}_j). \tag{2}$$

The distribution of particle core functions is effectively handled by the linear superposition of locally centered solutions of Poisson's equation. For a compact spherically-symmetric core function, $\sigma(\mathbf{r})$, the far field solution to Poisson's equation in 3D space, namely,

$$-\nabla^2\phi(\mathbf{x})=4\pi\sigma(\mathbf{x}), \tag{3}$$

can be approximated by a multipole expansion.[27] Here we use reduced units where nondimensional Gaussian units are implied. The multipole expansion, here stated in Cartesian coordinates ($\mathbf{x}\in\{x,y,z\}$) to be consistent with the literature, is given in its general form (a Legendre polynomial expansion is used in FMM),

$$\begin{aligned}\phi(\mathbf{x})=&\sum_{n=0}^{\infty}\sum_{l=0}^{n}\sum_{k=0}^{n-l}\frac{(-1)^n}{l!k!(n-l-k)!}\\ &\times\left\{\int\int\int x_0^l y_0^k z_0^{n-l-k}\sigma(x_0,y_0,z_0)dx_0dy_0dz_0\right\}\\ &\cdot\frac{\partial^n}{\partial x^l\partial y^k\partial z^{n-l-k}}\left[\frac{1}{r}\right]\quad\text{for } r>a;\end{aligned} \tag{4}$$

here $\mathbf{x}$ is interchangeable with $\mathbf{r}$. The integration above is contained in a volume inside the sphere $r=a$, within which all the charge resides. The truncation of the expansion has decreasing residual error for increasing radial values of $R$, $R^2=(x-x_0)^2+(y-y_0)^2+(z-z_0)^2$, where $r^2=x^2+y^2+z^2$. If the charge distribution is spherically symmetric, we expand around the center of charge and, since the integration of the odd terms vanish, we are left with the simplified form,

$$\phi(r)=\frac{A_\sigma}{r}+\frac{B_\sigma}{r^3}+\mathcal{O}\left(\frac{1}{r^5}\right), \tag{5}$$

where

$$A_\sigma=4\pi\int_\Omega\sigma(r)r^2\mathrm{d}r, \tag{6a}$$

$$B_\sigma=4\pi\int_\Omega\sigma(r)r^4\mathrm{d}r, \tag{6b}$$

and $\Omega$ is a volume containing the charge. After we normalize the core function to a unit net charge we have, $\tilde{\phi}(r)=A_\sigma^{-1}\phi(r\to\infty)\approx 1/r$; i.e., the normalized potential asymptotically approaches the Coulomb potential in the far field. We can rewrite the above expressions such that the Coulomb potential is split into two terms,

$$\frac{1}{r}=\frac{S(r)}{r}+\tilde{\phi}(r). \tag{7}$$

Here the switch function, $S(r)$, can be defined to be a decreasing function of $r$, i.e., the normalized potential, $\tilde{\phi}(r)$, has the same far field solution as $1/r$, namely,

$$S(r)/r = 1/r - A_\sigma^{-1}\phi(r) \sim \mathcal{O}\left(\frac{1}{r^p}\right), \quad p>1, \quad r\to\infty \tag{8}$$

or equivalently $S(r\to\infty)\approx 1/r^{p-1}$. Our goal is to define a suitable normalized core function that produces rapid decay of $S(r)$, expressed as

$$-\nabla^2\tilde{\phi}(r) = 4\pi\tilde{\sigma}(r) = 4\pi A_\sigma^{-1}\sigma(r), \tag{9}$$

$$S(r) = 1 - r\tilde{\phi}(r). \tag{10}$$

The Ewald Gaussian core function, $g(r,\beta)=\exp(-\beta^2 r^2)$, is ideal for this purpose. The solution of Poisson's equation subject to the unit normalized Gaussian right-hand side, for an unbounded domain, gives a decay in $S(r)$ that is faster than any algebraic power of $1/r$ [or first order exponential, $\exp(-\alpha k)$], i.e.,

$$\tilde{\sigma}(r;\beta) = \frac{\beta^3}{\pi^{3/2}}\exp(-\beta^2 r^2), \tag{11}$$

$$\tilde{\phi}(r) = (1-\mathrm{erfc}(r,\beta))/r, \tag{12}$$

$$S(r) = \mathrm{erfc}(r,\beta), \tag{13}$$

where $\mathrm{erfc}(r,\beta)$ is the complementary error function that decays as $\exp(-\beta^2 r^2)$ in the far field.

For a periodic lattice, we solve Poisson's equation, with a charge distribution given by Eq. (2), for periodic boundary conditions; the particle core and switch functions in the unit cell are extended periodically by linear superposition. For a general unit normalized core function $\tilde{\sigma}(r)$, we define the Fourier transform as

$$\hat{\sigma}(\mathbf{k}) = \int_\Omega d\mathbf{r}\tilde{\sigma}(\mathbf{r})\exp(-i\mathbf{k}\cdot\mathbf{r}). \tag{14}$$

Equivalently, we express its Fourier series as

$$\tilde{\sigma}(\mathbf{r}) = \frac{1}{V}\sum_{\mathbf{k}=-\infty}^{\infty}\hat{\sigma}(\mathbf{k})\exp(i\mathbf{k}\cdot\mathbf{r}), \tag{15}$$

where $V$ is volume of the cubic unit cell, $\mathbf{k}=2\pi\mathbf{n}/L$, $V=L^3$, $k=|\mathbf{k}|=2\pi|\mathbf{n}|/L$, and $\mathbf{n}=(n_x,n_y,n_z)$, $n_x,n_y,n_z$ are integers. The solution to Poisson's equation, Eq. (9), can be written as

$$\tilde{\phi}(\mathbf{r}) = \frac{4\pi}{V}\sum_{\mathbf{k}\neq 0}\frac{\hat{\sigma}(\mathbf{k})}{k^2}\sum_{j=1}^{N} q_j\exp(i\mathbf{k}\cdot(\mathbf{r}-\mathbf{r}_j)), \tag{16}$$

where $q_j$ is the net charge assigned to particle $j$ centered at a physical space coordinate $\mathbf{r}_j$.

For periodic applications, the Gaussian function has a highly favorable decay rate in its Fourier series expansion, i.e., faster than any algebraic power of $1/k$ (or first order exponential), namely,

$$\hat{g}(k,\beta) = \exp\left(-\frac{k^2}{4\beta^2}\right). \tag{17}$$

However, the Ewald formulation is limited, in the sense that only a one-dimensional optimization is possible—an adjustment of the Gaussian-width parameter $\beta$. To allow general spherically-symmetric core functions with flexible properties, we introduce additional degrees of freedom. We first solve Poisson's equation for a general $\sigma(r)$ in an unbounded domain. For a general spherically-symmetric core function $\sigma(r)$ in an unbounded domain, we solve Poisson's equation with established techniques from electrostatic theory[28] (see also Refs. 5 and 22). An integral equation for the solution of Poisson's equation, Eq. (3), with a spherically-symmetric core function is given as

$$\phi(r) = \frac{4\pi}{r}\int_0^r d\xi(\xi^2\sigma(\xi)) + 4\pi\int_r^\infty d\xi(\xi\sigma(\xi)). \tag{18}$$

To evaluate the periodic lattice sum, we must also have the Fourier transform of $\sigma(r)$ available. In principle, the transform can be computed numerically; however, an efficient computational formulation would likely require an analytical expression. For a normalized spherically-symmetric core function, the Fourier transform can be written as[6]

$$\hat{\sigma}(k,\beta) = \frac{4\pi}{k}\int_0^\infty u\tilde{\sigma}(u,\beta)\sin(ku)du. \tag{19}$$

The core function is normalized to guarantee a decay in the real space switch function.

The above formulation leads directly to the usual real/reciprocal space splitting for a periodic lattice summation,

$$\frac{1}{2}\sum_{i,j=1}^{N} q_i q_j {\sum_{|\mathbf{n}|}}' \frac{1}{|\mathbf{r}_{ij}+\mathbf{n}|} = E_{\mathrm{dir}} + E_{\mathrm{recip}} - E_{\mathrm{self}}, \tag{20}$$

$$E_{\mathrm{dir}} = \frac{1}{2}\sum_{i,j=1}^{N} q_i q_j {\sum_{|\mathbf{n}|}}' \frac{S(|\mathbf{r}_{ij}+\mathbf{n}|)}{|\mathbf{r}_{ij}+\mathbf{n}|}, \tag{21}$$

$$E_{\mathrm{recip}} = \frac{4\pi}{2V}\sum_{|\mathbf{k}|\neq 0}\frac{\hat{\sigma}(\mathbf{k})}{|\mathbf{k}|^2}P(\mathbf{k})P(-\mathbf{k}),$$

$$P(\mathbf{k}) = \sum_{j=1}^{N} q_j\exp[i\mathbf{k}\cdot\mathbf{r}_j], \tag{22}$$

$$E_{\mathrm{self}} = \frac{4\pi}{2}\sum_{i=1}^{N} q_i^2\int_0^\infty r\tilde{\sigma}(r,\beta)dr. \tag{23}$$

The first term ($E_{\mathrm{dir}}$) is the real space (direct) term; $E_{\mathrm{recip}}$ is the reciprocal space term, and $E_{\mathrm{self}}$ is the self-energy correction to the Poisson solution with a charge distribution given by Eq. (2) and stated for a spherically-symmetric core function; for further details, see Refs. 2, 6, and 29. For a more general unit cell, an additional term is added to the electrostatic energy per cell which depends on the net dipole moment of the unit cell and its geometry.[2,18,29,30]

For nonperiodic particle simulations, the splitting remains valid and we must solve Poisson's equation for a multicentered charge density with appropriate far field boundary conditions. Nonperiodic solutions with regards to lattice sums have been recently addressed in Refs. 31 and 32. For mixed periodic and nonperiodic charge densities, Poisson's solution can be efficiently computed by rapidly converging

spectral methods, recently introduced within the context of electronic structure calculation;[33,34] such methods offer an alternative to the Fourier series expansion.

## III. OPTIMAL CORE FUNCTIONS

### A. Overview

Core functions other than Ewald's Gaussians, tailored to specific applications, are the subject here. We briefly review below the necessary requirements for an efficient lattice summation. Given a core function, $\sigma(r)$, that decays suitably fast [which implies a rapid decay of $S(r)$], we derive a solution of Poisson's equation on an infinite domain, $\phi(r)$, and thus a switch function,

$$S(r)=1-r\tilde{\phi}(r) \tag{24}$$

for use in an Ewald-type splitting. For the formulation to be competitive relative to the Ewald method, $S(r)$ should decay as $\exp(-\beta^2 r^2)$ and thus can be evaluated by appropriate truncation. For the reciprocal term, the Fourier transform of $\sigma(r)$, namely $\hat{\sigma}(k)$, must decay suitably fast in reciprocal space to maintain an efficient solution to Poisson's equation in a periodic lattice. To remain competitive to the Ewald method, $\hat{\sigma}(k)$ should decay as $\exp(-k^2/4\beta^2)$. The rapid decay of $\hat{\sigma}(k)$ reflects the smoothness of the core function and ultimately states the well established fact from approximation theory[35] that the Fourier series of the periodic extension of an ''infinitely'' smooth function decays faster than any algebraic power of $k$; the Gaussian is exceptional in this regard since it decays faster than any first order exponential function. For nonperiodic lattice sums, the rapid decay of $\hat{\sigma}(k)$ is a favorable property since it implies that the gradients are not large in magnitude; thus, a standard grid method, such as finite elements or spectral elements, requires less resolution. The underlying goal of a well formulated core function is a large degree of smoothness in the solution of Poisson's equation, subject to a charge distribution given by Eq. (2), while maintaining a rapid physical space decay in the switch and core functions.

Studies on several non-Gaussian core functions, which include functions with rigid cutoffs, can be found in Refs. 5, 15, and 22. We do not expect rigid cutoff formulations to be competitive relative to the Ewald method since their nonsmooth character will lead to algebraic convergence in the Fourier series expansion of $\sigma(r)$; truncated polynomial core functions have recently been examined in Ref. 36. Likewise, the exponentially converging core functions studied in Ref. 5 ($\exp(-\alpha r)$) are not expected to be competitive with Ewald's method since their Fourier series decay with algebraic rates as well.

### B. Core functions and integral evaluations

A class of core functions that retain the favorable properties of the Ewald Gaussian is given by

$$\sigma(r;\beta,n)=A_n r^{2n}\exp(-r^2\beta^2),\quad n=0,1,2,\ldots, \tag{25}$$

where $A_n^{-1}=4\pi\int_0^\infty r^{2n+2}\exp(-\beta^2 r^2)dr$ is a normalizing constant. The Fourier transform given by Eq. (19) is obtained from known definite integrals[37]

$$\int_0^\infty x^{2n+1}\exp(-\beta^2 x^2)\sin(ax)$$

$$=(-1)^n\frac{\sqrt{\pi}}{(2\beta)^{2n+2}}\exp\left(-\frac{a^2}{4\beta^2}\right)\mathrm{H}_{2n+1}\left(\frac{a}{2\beta}\right), \tag{26}$$

which gives

$$\hat{\sigma}(k;\beta,n)=\frac{4\pi A_n}{k}(-1)^n\frac{\sqrt{\pi}}{(2\beta)^{2n+2}}$$

$$\times\exp\left(-\frac{k^2}{4\beta^2}\right)\mathrm{H}_{2n+1}\left(\frac{k}{2\beta}\right). \tag{27}$$

Here the functions $\{\mathrm{H}_{2n+1}(x)\}$ are the odd Hermite polynomials.

The integral expressions involved in Eq. (18) are routinely obtained as well. In Appendix A we derive recursion relations for the fast evaluation of the switch functions associated with $\sigma(r;\beta,n)$. The first three switch functions (corresponding to $n=0,1,2$) are

$$S(r;\beta,0)=\mathrm{erfc}(\beta r), \tag{28a}$$

$$S(r;\beta,1)=\mathrm{erfc}(\beta r)+4\pi A_1\exp(-\beta^2 r^2)\frac{r}{(2\beta^2)^2}, \tag{28b}$$

$$S(r;\beta,2)=\mathrm{erfc}(\beta r)+4\pi A_2\exp(-\beta^2 r^2)$$

$$\times\left(\frac{r^3}{(2\beta^2)^2}+\frac{(5\cdot 3-4\cdot 2)r}{(2\beta^2)^3}\right), \tag{28c}$$

where $A_1^{-1}=(4\cdot 3)\pi^{3/2}/(2\beta^2)^2 2\beta$ and $A_2^{-1}=(4\cdot 5\cdot 3)\pi^{3/2}/(2\beta^2)^3 2\beta$; see Appendix A for detailed derivations.

Though for $n>0$ the switch function and Fourier transform of the core function both converge slower than the Ewald method ($n=0$), they converge faster than any first-order exponential. The usefulness of the core functions emerges from the functions' series expansion,

$$\sigma(r;\beta)=\sum_{i=0}^{n} a_i A_i r^{2i}\exp(-r^2\beta^2). \tag{29}$$

The only constraint imposed on the series, Eq. (29), is a normalization condition that enforces $\Sigma_i^n a_i=1$; the coefficients $a_i$ are found from a suitably chosen optimization statement based on functionals derived from either the switch function or Fourier transform. Both the Fourier transform and the switch function are linear operations and after optimization are given as

$$\hat{\sigma}(k;\beta)=\sum_{i=0}^{n} a_i\hat{\sigma}(k;\beta,i), \tag{30}$$

$$S(r;\beta)=\sum_{i=0}^{n} a_i S(r;\beta,i). \tag{31}$$

The coefficients can be computed to design core functions that approximate the function $f(r)\exp(-r^2\beta^2)$, where $f(r)$ is an even function of $r$.

## IV. OPTIMIZATION STATEMENTS

### A. Pairwise interaction splitting

We are interested in tailoring the Ewald splitting to applications of MTS integration in molecular dynamics simulations. Other time integration strategies such as symplectic mixed implicit-explicit methods[38] can also benefit from our tailored formulation. In MTS schemes, the various force components governing the particle's motion are split based on their time scales; i.e., slower force components are evaluated less frequently.[26] Our recent application of MTS to PME formulations[25,39] has revealed a severe limitation on the largest possible timestep. That is, the updating frequency of the reciprocal term (considered to be the ''slow force'') cannot be too large.[25] This is not surprising since the reciprocal term in the Ewald formulation has fast components associated with near-field particle separations, along with its isolated long-range interactions. Recently, Procacci *et al.*[40] have investigated the limitations of the fast component of the Ewald reciprocal term on MTS schemes and found outer timestep limitation of approximately 8 fs, which is in agreement with our PME studies.[25]

Our goal of isolating all near-field particle interactions into the real space sum—a spatial separation—is expected to translate to a temporal separation—isolating the fastest time scales of the electrostatics in the direct (real) space sum.

We begin the construction by simply noting that the switch function offers an opportunity to formulate a core function that isolates near and far field interactions into the real and reciprocal space terms, respectively. The reciprocal and real space potentials and their respective force components, $\mathbf{F}(r)=-\nabla U(r)$, are

$$U_{\text{recip}}=\frac{1}{r}(1-S(r)), \tag{32}$$

$$U_{\text{dir}}=\frac{S(r)}{r}, \tag{33}$$

$$\mathbf{F}_{\text{recip}}=\frac{\mathbf{x}}{r^3}(1-S(r))-\frac{\mathbf{x}}{r^2}\frac{dS(r)}{dr}, \tag{34}$$

$$\mathbf{F}_{\text{dir}}=\frac{\mathbf{x}}{r^3}S(r)+\frac{\mathbf{x}}{r^2}\frac{dS(r)}{dr}, \tag{35}$$

where $\mathbf{x}$ is the coordinate vector; $\mathbf{x}=(x\mathbf{u}_x,y\mathbf{u}_y,z\mathbf{u}_z)$ with unit vectors $\mathbf{u}_i$. We note that a core function that results in a switch function with the form,

$$S_c(r)=\begin{cases}1 & r\leqslant r_c\\ 0 & r>r_c\end{cases}$$

has no force or potential contribution associated with the reciprocal term for $r<r_c$. A switch function with this stepwise character will effectively isolate the near-field pairwise interaction in the real space sum and meet our desired goal. Alternatively, to isolate the near-field interaction [or make $\mathbf{F}_{\text{recip}}$ vanish, i.e., Eq. (34)] the switch function need only be equal to 1 and have $dS(r)/dr=0$ for $r\leqslant r_c$; for $r>r_c$ the switch function $S(r)$ can be nonzero.

#### 1. Inverse statement

With the series expansion associated with Eq. (31), we optimize the coefficients $a_i$ to match a desired switch function. A least-squares fit to the switch function is given by the linear algebra statement,

$$M_{ij}a_j=b_i, \tag{36}$$

where

$$M_{ij}=\int_0^\infty drS(r;\beta,i)S(r;\beta,j),\quad b_i=\int_0^\infty drS(r;\beta,i)S_c(r).$$

The series expansion is not expected to converge at the discontinuity due to the smooth basis-set associated with the $S(r;\beta,i)$ functions, i.e., a Gibb's phenomena will be present at the step interface. A modified least-squares statement is recommended for the near-field target switch function, $S_c(r)=1.0$, where the integration is taken over a region $r<2.5$ units. By utilizing the normalization constraint, $\Sigma_i^n a_i=1$, on the coefficients of the expansion for the switch function, i.e.,

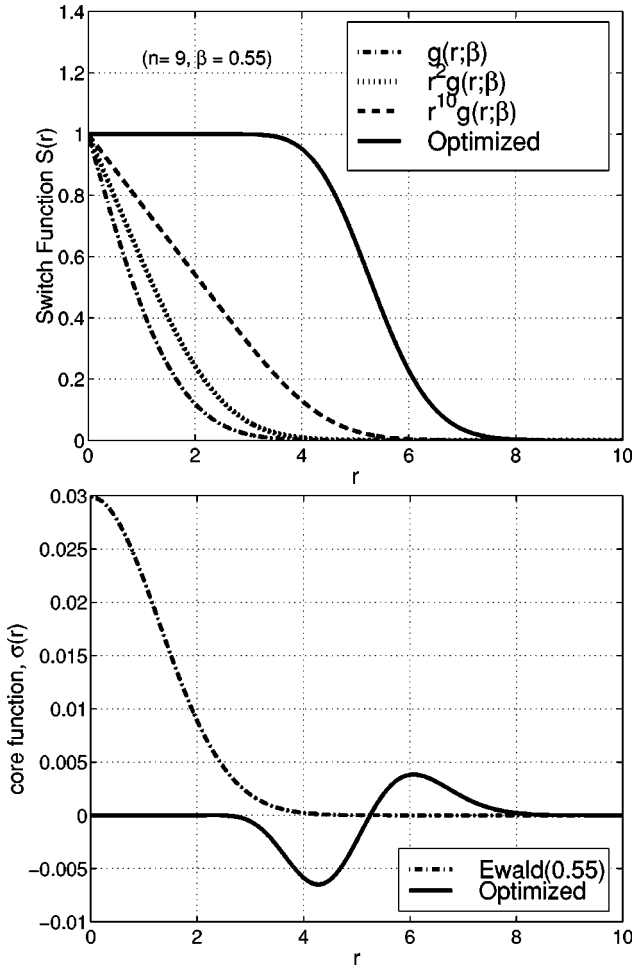


FIG. 1. (Top) the optimized switch function designed to isolate the near-field pairwise interaction in the real space sum is compared to the Ewald solution and several radial weighted functions ($\beta=0.55$). (Bottom) the core function resulting from the pairwise particle splitting is plotted along with the Ewald core function at the same $\beta$ value.

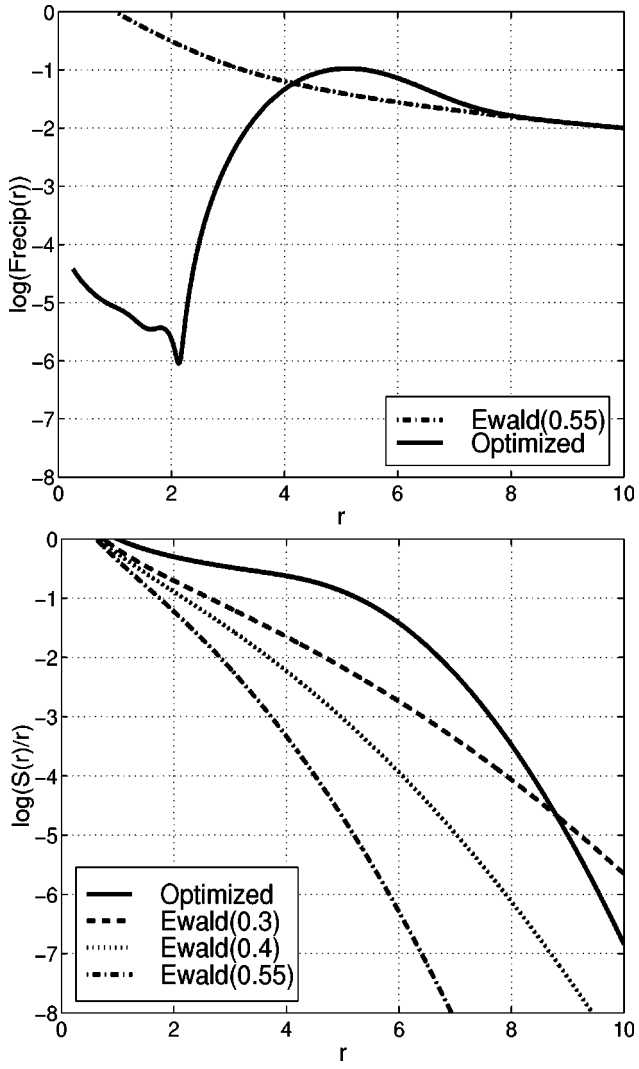


FIG. 2. (Top) the logarithm of reciprocal force component for the two-particle interaction. (Bottom) the logarithm of $S(r)/r$. Here the switch function is optimized to minimize the reciprocal force for near-field particle separations with $\beta=0.55$; a comparison is shown to the Ewald method with the same $\beta$ value.

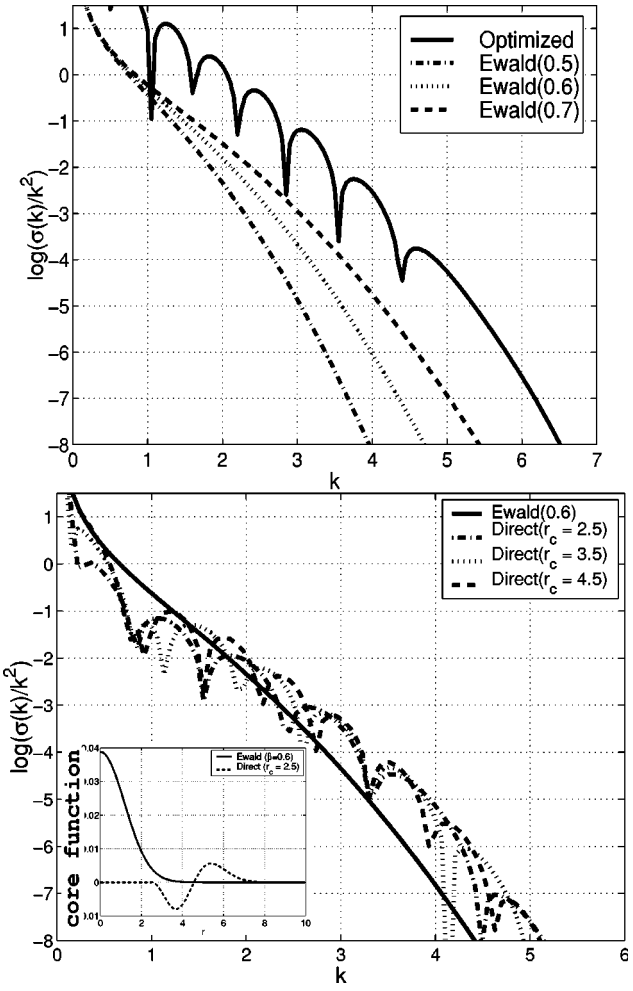


FIG. 3. (Top) the spectrum of Poisson kernel is shown for the optimization of the pairwise interaction splitting. Here the switch function $S(r)$ is optimized to isolate the near-field interaction in the real space sum. Several Ewald solutions are presented for similar $\beta$ values, the optimized solution was constructed with $\beta=0.55$. (Bottom) the direct formulation ($\beta=0.6$) is used for the pairwise interaction splitting and the decay of the Poisson kernel is plotted for several different cutoff values ($r_c=2.5$, 3.5, and 4.5) along with the core function for $r_c=2.5$ in the lower left corner.

$$S(r,\beta)=\sum_{i=0}^{n} a_i \operatorname{erfc}(\beta r)+a_i p_i \exp(-\beta^2 r^2), \tag{37}$$

we are left with an equivalent approximation for $S(r,\beta)\approx 1$ in the near-field region as

$$\operatorname{erf}(\beta r)\approx\sum_{i=1}^{n} a_i p_i(r)\exp(-\beta^2 r^2); \quad \text{for } r<r_c,\ a_0=0, \tag{38}$$

$$p_i(r)=4\pi A_i(P_{2i+2}(r)-rP_{2i+1}(r)). \tag{39}$$

Here $p_i(r)$ are the odd polynomials obtained from the recursion relation associated with the polynomials $P_i(r)$ derived in Appendix A for the switch functions. The rapid decay in the switch, $\sim\exp(-\beta^2 r^2)$, is contained within our basis-set and will maintain the well localized core and switch function for efficient implementation of this new lattice sum formulation.

In Fig. 1 we present the switch and core functions resulting from an expansion with $n=9$ terms in our least-squares fit with $\beta=0.55$. Figure 2 plots the the logarithm of the reciprocal force and $S(r)/r$. The above results are encouraging for isolating the near-field force into the real space sum. The results indicate that the new core function, posed as an inverse problem, captures the desired features of a pairwise interaction splitting for the lattice sum formulation. For the $\beta=0.55$ case, the practical real space sum cutoff values are below 10 radial units and negligible reciprocal forces are maintained to approximately 3 radials units.

For an effective lattice summation, we must also examine the effect of the optimization on the rate of decay of the Fourier spectrum for the core function. In Fig. 3(a) we plot the logarithm of the Poisson kernel for the $(n,\beta)=(9,0.55)$ approximation. The error of a given $k$ vector is larger than an equivalent Ewald $\beta$ value; however, the decay is still rapid and faster than any first order exponential.

### 2. Direct statement

Our core function above is qualitatively zero up to a certain cutoff value and then has a single wavelike shape (Fig. 1). The associated numerical error is small, as shown in Fig. 2. Guided by these encouraging results, we analyze a core function with these features and present an exact statement for the pairwise interaction splitting.

Note that a switch function Eq. (24) meets the desired pairwise interaction splitting if the potential $\phi(r)$ is zero (or S=1) for $r \leqslant r_c$. From Eq. (18), we see that $\phi(r)$ is zero for $r \leqslant r_c$ if the core function is given by

$$\sigma(r)=\begin{cases} 0 & r \leqslant r_c \\ \sigma(r-r_c) & r>r_c \end{cases} \tag{40}$$

and obeys the constraint

$$\int_{r_c}^{\infty} r\sigma(r)dr=0. \tag{41}$$

This is also the qualitative form of the core function found from our optimization above. A core function that can be designed to meet this exact pairwise interaction splitting is given by our polynomial/Gaussian expansion,

$$\sigma(r)=\begin{cases} 0 & r \leqslant r_c \\ (a_1A_1(r_c)(r-r_c)^2+a_2A_2(r_c)(r-r_c)^4), & \\ \quad \times \exp(-\beta^2(r-r_c)^2) & r>r_c \end{cases} \tag{42}$$

where $a_1$ and $a_2$ are coefficients, and $A_2(r_c)$ and $A_4(r_c)$ are normalizing constants for the basis core functions. We must now satisfy the two constraints,

$$a_1+a_2=1, \tag{43a}$$

$$C_1A_1(r_c)a_1+C_2A_2(r_c)a_2=0. \tag{43b}$$

The first constraint satisfies the normalization condition, and the second ensures the splitting condition Eq. (41), i.e.,

$$C_i=\int_{r_c}^{\infty} r(r-r_c)^{2i}\exp(-\beta^2(r-r_c)^2)dr. \tag{44}$$

The solution for $a_i$ can be found from the linear algebraic statement,

$$a_1=C_2A_2(r_c)/(C_2A_2(r_c)-C_1A_1(r_c)), \tag{45a}$$

$$a_2=-C_1A_1(r_c)/(C_2A_2(r_c)-C_1A_1(r_c)). \tag{45b}$$

The normalization constants $A_1(r_c)$ and $A_2(r_c)$ are given in Eq. (52) and Eq. (53) below, and the constants $C_i$ are readily obtained through their definite integrals (see Appendix B),

$$C_i=P_{2i+1}(0)+r_c\frac{A_{i-1}^{-1}}{4\pi}, \quad i=1,2,3,\ldots, \tag{46}$$

where $A_i^{-1}$ and $P_n(0)$ are given in Appendix A. Evaluating these expressions leads to

$$C_1=\frac{2}{(2\beta^2)^2}+r_c\frac{\sqrt{\pi}}{4\beta^3}, \tag{47a}$$

$$C_2=\frac{8}{(2\beta^2)^3}+r_c\frac{3\sqrt{\pi}}{8\beta^5}. \tag{47b}$$

Evaluating Eq. (18) for the potential $\phi(r)$ defines our switch function. The Fourier transform is solved by evaluating Eq. (19) for the shifted core function so that the reciprocal term can be evaluated. The piecewise smooth character of the core function does not effect the rapid decay of the Possion kernel in reciprocal space or the rapid decay of the switch function in physical space. Both favorable properties of the Ewald method are retained. We defer the derivations to Appendix B and present the results here.

The solution of Poisson's equation, Eq. (3), for the piecewise smooth core function is an exercise in integral calculus. In Appendix B we establish the detailed formulations for a core function given by

$$\sigma(r;\beta,r_c,n)=\begin{cases} 0 & r \leqslant r_c \\ (r-r_c)^{2n}\exp(-\beta^2(r-r_c)^2) & r>r_c \end{cases}, \quad n=1,2,3,\ldots. \tag{48}$$

For the core functions $\sigma(r;\beta,r_c,1)$ and $\sigma(r;\beta,r_c,2)$ we have $\phi(r;\beta,r_c,n)=0$ for $r \leqslant r_c$, and for $r>r_c$ we have

$$\begin{aligned}\phi(r;\beta,r_c,1)=&\frac{(A_1^{-1}+r_c^2A_0^{-1})\operatorname{erf}(\beta u)+4r_c/(2\beta^2)^2}{r}\\ &-\frac{\exp(-\beta^2u^2)}{r}[P_4(u)+2r_c(u^2/(2\beta^2)\\ &+2/(2\beta^2)^2)+r_c^2P_2(u)]+P_3(u)\\ &\times\exp(-\beta^2u^2)+r_c\left[\frac{u}{2\beta^2}\exp(-\beta^2u^2)\right.\\ &\left.+\frac{\sqrt{\pi}}{2\beta(2\beta^2)}\operatorname{erfc}(\beta u)\right],\end{aligned} \tag{49}$$

$$\begin{aligned}\phi(r;\beta,r_c,2)=&\frac{(A_2^{-1}+r_c^2A_1^{-1})\operatorname{erf}(\beta u)+16r_c/(2\beta^2)^3}{r}\\ &-\frac{\exp(-\beta^2u^2)}{r}[P_6(u)+2r_c(u^4/(2\beta^2)\\ &+4u^2/(2\beta^2)^2+8/(2\beta^2)^3)+r_c^2P_4(u)]\\ &+P_5(u)\exp(-\beta^2u^2)\\ &+r_c\left[\left(\frac{u^3}{2\beta^2}+\frac{3u}{(2\beta^2)^2}\right)\exp(-\beta^2u^2)\right.\\ &\left.+\frac{3\sqrt{\pi}}{2\beta(2\beta^2)^2}\operatorname{erfc}(\beta u)\right],\end{aligned} \tag{50}$$

where $u=r-r_c$. Next, we define the appropriate normalization of the core functions so that the switch functions will decay to zero in the far field. In the far field, the first terms in Eqs. (49) and (50) dominate and are given by

$$\phi(r\to\infty;\beta,r_c,1)\approx \frac{A_1^{-1}+r_c^2A_0^{-1}+4r_c/(2\beta^2)^2}{r} + \mathcal{O}\left(\frac{\mathrm{erfc}(\beta r)}{r}\right), \tag{51a}$$

$$\phi(r\to\infty;\beta,r_c,2)\approx \frac{A_2^{-1}+r_c^2A_1^{-1}+16r_c/(2\beta^2)^3}{r} + \mathcal{O}\left(\frac{\mathrm{erfc}(\beta r)}{r}\right), \tag{51b}$$

respectively.

The normalization that guarantees that the switch function will decay as $\exp(-\beta^2r^2)$ in the far field is therefore,

$$A_1(r_c)=1/(A_1^{-1}+r_c^2A_0^{-1}+4r_c/(2\beta^2)^2), \tag{52}$$

$$A_2(r_c)=1/(A_2^{-1}+r_c^2A_1^{-1}+16r_c/(2\beta^2)^3). \tag{53}$$

Lastly, we arrive at a switch function that defines the pairwise interaction splitting for the core function given in Eq. (42),

$$S(r;\beta,r_c)=\begin{cases} 1 & r\leqslant r_c \\ 1-ra_1A_1(r_c)\phi(r;\beta,r_c,1) & \\ \quad -ra_2A_2(r_c)\phi(r;\beta,r_c,2) & r>r_c\,. \end{cases} \tag{54}$$

The core, switch, and potential functions are piecewise smooth; they are also continuous by construction at $r=r_c$: $\{\sigma(r),S(r),\phi(r)\}\in C^0$; it can also be established that $\{S(r),\phi(r)\}\in C^1$ at $r=r_c$.

The Fourier transform of the core function given in Eq. (48) is readily found from a change of variables and known definite integrals (see Appendix B) to result in

$$\hat{\sigma}(k;\beta,r_c,n)=\frac{4\pi}{k}\exp\left(-\frac{k^2}{4\beta^2}\right)\left[\left(\cos(kr_c)\frac{(-1)^n\sqrt{\pi}}{(2\beta)^{2n+2}} + \sin(kr_c)\frac{\Gamma(n+1)}{2^{2n+2}\beta^{n+1}}\right)\mathrm{H}_{2n+1}\left(\frac{k}{2\beta}\right) + \left(r_c\cos(kr_c)\frac{\Gamma(n+1)}{2^{2n}\beta^n} + r_c\sin(kr_c)\frac{(-1)^n\sqrt{\pi}}{(2\beta)^{2n+1}}\right)\mathrm{H}_{2n}\left(\frac{k}{2\beta}\right)\right]. \tag{55}$$

The Fourier transform of the total core function is therefore

$$\hat{\sigma}(k;\beta,r_c)=a_1A_1(r_c)\hat{\sigma}(k;\beta,r_c,1)+a_2A_2(r_c)\hat{\sigma}(k;\beta,r_c,2). \tag{56}$$

Note that we have effectively established a reciprocal-space filter which incorporates the pairwise interaction splitting into the periodic lattice, i.e.,

$$\hat{\sigma}(k;\beta,r_c)=F(k;\beta,r_c)\hat{\sigma}_{\mathrm{Ewald}}(k;\beta), \tag{57a}$$

$$\hat{\sigma}_{\mathrm{Ewald}}(k;\beta)=\exp\left(-\frac{k^2}{4\beta^2}\right), \tag{57b}$$

where $F(k;\beta,r_c)$ is readily established from the above expressions.

In Fig. 3(b) we plot the Poisson kernel for the direct pairwise interaction formulation for $\beta=0.6$ and cutoff values $r_c$ of 2.5, 3.5, and 4.5. The results show that the decay of the reciprocal-space sum is insensitive to the cutoff value; furthermore, the decay of the large $k$ vectors at $\beta=0.6$ is bounded by the Ewald ($\beta=0.7$) result. As compared to the inverse statement for $\beta=0.55$ [Fig. 3(a)], we have a favor able reciprocal-space decay rate with our higher $\beta=0.6$ value. The oscillations in the Poisson kernel are somewhat explained by Eq. (55) since sine and cosine functions are apparent in the formulation. The core function derived with the direct formulation, for $\beta=0.6$ and $r_c=2.5$, is also plotted in Fig. 3(b); we see qualitatively the same functional form found from the inverse statement.

Lastly, we note that the core function that results in a minimal departure from the traditional Ewald formulation, and that satisfies the necessary continuity conditions, is given by

$$\sigma(r)=\begin{cases} 0 & r\leqslant r_c \\ (a_1A_1(r_c)(r-r_c)+a_2A_2(r_c)(r-r_c)^2) & \\ \quad\times\exp(-\beta^2(r-r_c)^2) & r>r_c\,. \end{cases} \tag{58}$$

We present the resulting potentials, transforms, and coefficients in Appendix C for the core function given in Eq. (58).

### B. Multilevel splitting of the pairwise interaction

The analysis above establishes a systematic way of formulating a two-level splitting of the Coulomb potential so that the two force components separate the near-field and far field interactions. Within the context of biomolecular dynamics, there is a hierarchy of time scales associated with the force field potentials; optimal MTS schemes[34] generally require a separation of temporal scales so that the various force components can be grouped into comparable dynamical ranges. Typically, a three level force splitting MTS scheme is used and each level is integrated with a different timestep. The Coulomb potential has a wide range of time scales that are not generally well separated. It would therefore be advantageous to have a procedure that would split the electrostatic potential into a hierarchy of scales that is more compatible with the nonelectrostatic force field potentials.

Formulating the Ewald-type method such that the reciprocal term has a negligible (or zero) force contribution for a pairwise interaction $\lesssim 4$ Å is a first step to multilevel time scale separation. However, the fastest modes in molecular dynamics are associated with bonded interactions (particle separations of $\approx 1-1.5$ Å). The next level of time scales occurs for hydrogen bonds and nearby nonbonded terms (e.g., pairwise separations of $\approx 2.5-4.5$ Å). It would therefore be desirable to further split the Coulomb term to more optimally match the molecular midfield interaction time scales.

We proceed by noting that our formulation above isolates the near and midfield pairwise interaction into the real space sum. The separation of the bonded particle separation and the midfield interactions from the real-space sum can be accomplished by introducing a new switch function, $S_1(r)$, where the original switch function is given by $S_2(r)$,

$$\frac{1}{r}=\frac{S_1(r)}{r}+\frac{S_2(r)-S_1(r)}{r}+\phi_{\text{recip}}(r). \tag{59}$$

The reciprocal potential, $\phi_{\text{recip}}(r)$, is the normalized potential stated in Eq. (7) and remains unmodified; its convergence rate remains dictated by the $S_2(r)$ parameters. The construction of the new switch function is formally the same as the original function; however, it is constructed for a pairwise interaction cutoff that is considerably shorter than the original; i.e.,

$$S_1(r)=\begin{cases}1 & r\leqslant r_{c1}<r_{c2}\\ =0 & r>r_{c1},\end{cases}$$

where $r_{c2}$ is the designed cutoff for the original switch function. This switch function, which is equal to 1, has a zero derivative with respect to $r$ and isolates all Coulombic interactions in its respective region. We force $S_1(r)$ to decay rapidly at the desired pairwise separation by following the procedure outlined in the previous section and choosing a large relative $\beta$. In Fig. 4, we present a switch function $S_1(r;\beta=2.6,\, n=13)$ formulated from a defined cutoff of $r_{c1}=1.25$ radial units, and an original pairwise interaction splitting that was constructed from $S_2(r)=\Sigma_{i=3}^{8}a_iS_2(r;\beta=0.6,i)$ with a cutoff of $r_{c2}=3.0$ radial units. Figure 4 illustrates the desired goal of defining a systematic procedure for multilevel pairwise interaction splitting through well defined analytical functions.

### C. Optimized convergence in reciprocal space

In Sec. III A we optimized the core function subject to the minimization of a functional relative to a desired property in the switch function. The same type of minimization can be established with respect to the Fourier transform of the core function. From Eqs. (30) and (27), we have

$$k\hat{\sigma}(k;\beta)=\sum_{i=0}^{n}4\pi a_iA_i(-1)^i\frac{\sqrt{\pi}}{(2\beta)^{2i+2}}\times\exp\left(-\frac{k^2}{4\beta^2}\right)\text{H}_{2i+1}\left(\frac{k}{2\beta}\right). \tag{60}$$

By taking $x=k/2\beta$ and $\hat{\sigma}(k;\beta)=f(x)$ we arrive at

$$xf(x)=\sum_{i=0}^{n}b_i\hat{\text{H}}_{2i+1}(x)\exp(-x^2), \tag{61}$$

where $f(x)$ is an even function of $x$, $b_i=(-1)^i4\pi^{3/2}a_ih_{2i+1}A_i/(2\beta c_i)$, $h_i$ is the constant of normalization for the Hermite polynomials $h_i=(\sqrt{\pi}2^ii!)^{1/2}$, $\hat{H}_{2i+1}(x)$ are the normalized Hermite polynomials, and $c_i=(2\beta)^{2i+2}$. Furthermore, we know from approximation theory that this weighted Hermite polynomial expansion is convergent if $f(x)$ is integrable; the expansion converges at an exponential rate if $xf(x)$ is smooth and all its derivatives satisfy

$$xf(x)=\mathcal{O}(\exp(\alpha x^2)),\quad |x|\to\infty \tag{62}$$

for some $\alpha<-1/2$.[35] With this result, we can optimize the Fourier transform of $\hat{\sigma}(k;\beta)$ so that its decay rate will be faster than the Ewald($\beta$) method, i.e., $\hat{\sigma}(k;\beta)\approx\hat{\sigma}(k;\beta_{\text{opt}}<\beta,0)$, while maintaining the rapid physical space decay, $\exp(-\beta^2r^2)$, of the switch and core functions. The orthogonal property of the Hermite polynomials makes the coefficients of the expansion easily defined by

$$b_i=2\int_0^\infty xf(x)\hat{\text{H}}_{2i+1}(x)dx, \tag{63}$$

where

$$\hat{\sigma}(k;\beta)=\frac{2\beta}{k}\sum_{i=0}^{n}b_i\hat{\text{H}}_{2i+1}\left(\frac{k}{2\beta}\right)\exp\left(-\frac{k^2}{4\beta^2}\right), \tag{64}$$

$$a_i=(-1)^i2\beta c_ib_ih_{2i+1}^{-1}/(4\pi^{3/2}A_i). \tag{65}$$

The core and switch functions are defined by the coefficients $a_i$, Eq. (29), and Eq. (31).

The scaling is taken such that a target function of $f(x)=\exp(-x^2)$ recovers the Ewald formulation in a one-term expansion. Here we examine a decay in the Fourier spectrum given by the function,

$$f(x;\alpha)=\exp(-\alpha x^2). \tag{66}$$

There are many possible optimized functions subject to the criteria that $f(x)<\exp(-x^2)$ and that $f(x)$ is smooth; $\alpha>1$ insures a faster decay of the Fourier spectrum relative to the Ewald formulation at the same $\beta$ value. The greater $f(x)$ deviates from the Ewald function, the greater number of terms are required in the series expansion to approximate $f(x)$ to a sufficient accuracy. For numerical implementations of Poisson's equation with accuracies given by $\hat{\sigma}(k;\beta)/k^2>10^{-5}$, we found that a modest approximation to $f(x)$ suffices. The coefficients typically result in a minimization that closely meets the $\Sigma_{i=0}^{n}a_i=1$ constraint and therefore a rescaling of the coefficients can be made after the minimization.

In general, we found that a least-squares fit on the region of the $x$ line of interest gave robust results; Fig. 5 presents the optimized and Ewald Poisson Kernel, $\hat{\sigma}(k;\beta)/k^2$, for the target function $f(x;\alpha=1.7,n=13,\beta=0.98)$ along with the Ewald ($\beta=0.5,0.6,0.7$) spectrum. The results of the optimized Fourier spectrum are encouraging and indicate that a

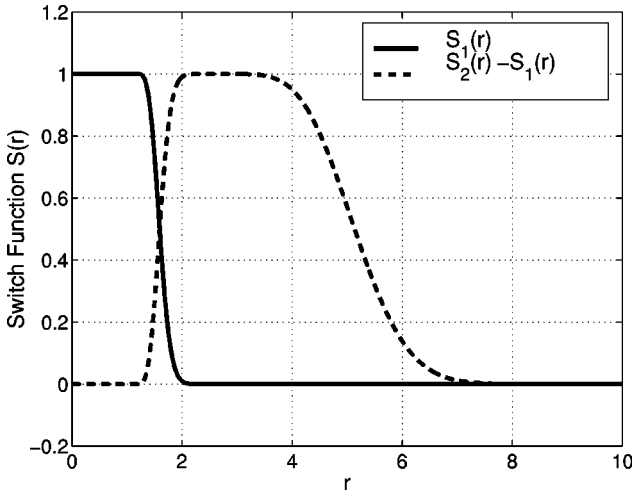


FIG. 4. The switch functions associated with a multi-level pairwise interaction splitting. The switch function $S_2(r)$ was formulated to isolate all near field interactions below $\approx 3$ radial units. The switch function $S_1(r)$ is optimized to isolate the near-field interactions below $\approx 1.25$ radial units.

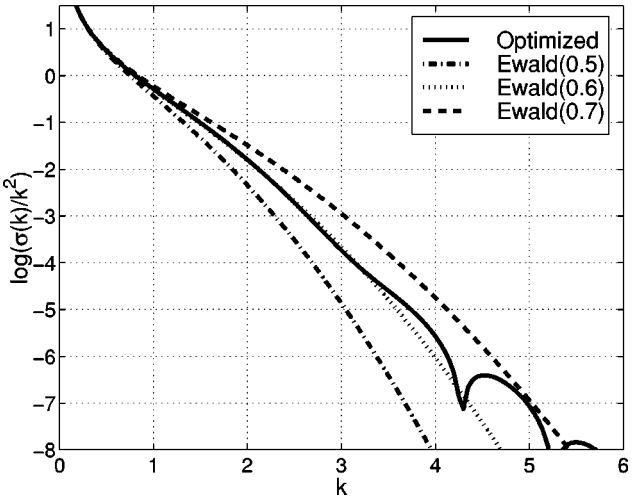


FIG. 5. The spectrum of Poisson kernel $\hat{\sigma}(k;\beta)/k^2$ as a result of the optimization of the Fourier spectrum decay rate. Here the Fourier transform of the core function is approximated by the function $f(x;\alpha)=\exp(-\alpha x^2)$. A least squares fit is made on the line $|k|<5.5$ with $(\alpha,\beta,n)=(1.7, 0.98, 13)$ and comparison is made to several Ewald solutions. The Ewald formulation is equivalent to $\alpha=1.0$ within the normalization used here.

large $\beta$ (e.g., $\beta=0.98$) can maintain a reciprocal space decay roughly equivalent to the Ewald ($\beta=0.6$) spectrum. The particle core function, reciprocal force, and the logarithm of the $S(r)/r$ function are given in Fig. 6 The decay of the $S(r)/r$ function indicates that the real space cutoff is approximately equivalent to the Ewald ($\beta=0.7$) result. Thus the new core function has a reciprocal space decay equivalent to a Ewald ($\beta=0.6$) result and a real space decay equivalent to the Ewald ($\beta=0.7$); i.e., a more efficient lattice sum than Ewald ($\beta=0.6$).

The decay rate of the Fourier spectrum at larger $k$ depends on the size of the expansion. Larger expansions offer better approximations to the rapidly decaying target function and a more accurate fit at higher $k$ values. However, a larger series expansion leads to a larger effective real space cutoff due to the higher degree polynomial; the $\exp(-\beta^2 r^2)$ term will always dominate the polynomial at sufficient radial distances. For larger $\beta$ values, where a relatively small cutoff value is found, we are interested in maintaining rapid decay in the reciprocal space by the optimization. In Fig. 7 we present the Poisson kernel and logarithm of $S(r)/r$ for the target functions $f(x;\alpha=3.0,n=19,\beta=1.25)$ and $f(x;\alpha=3.0,n=14,\beta=1.25)$. The $n=14$ optimization offers a slightly reduced decay rate of the Poisson kernel for large $k$ but an improved real-space decay with lower effective cutoff.

## V. SUMMARY

We have examined the formulation of specialized splittings of a lattice sum through two optimization statements. Both formulations were cast in an Ewald-type approach where the Coulomb potential is split into a real space sublattice and a second term which is the solution of Poisson's equation. In the first case, a core function and its Fourier transform, were formulated to establish a pairwise interaction splitting, namely the reciprocal potential and its force must vanish when particle separations are less than a specified value. This splitting was studied through an inverse statement (Sec. IV A 1), where the switch function was optimized, and a direct statement (Sec. IV A 2) where an exact pairwise interaction splitting was recovered. The direct statement offers favorable properties with respect to the inverse statement and is currently being evaluated for application in biomolecular dynamics simulation. An interesting outcome of the pairwise interaction splitting is that the core functions exhibit no self-interaction and if the cutoff value, $r_c$, is larger than the distance between bonded pairs in a molecular dynamics simulation, there is no need for the addition of an exclusion sum to correct the reciprocal term.

The second optimization statement was directed at minimizing the reciprocal space convergence rate relative to a rapidly decaying Fourier transform. The optimization of the Fourier spectrum decay rate demonstrated an improvement over the Ewald method, where a lower real space cutoff value was achieved while maintaining a favorable reciprocal space decay rate.

In both optimizations, the core function and its Fourier transform were given by a series expansion, namely a Gaussian function multiplied by a polynomial. The core function

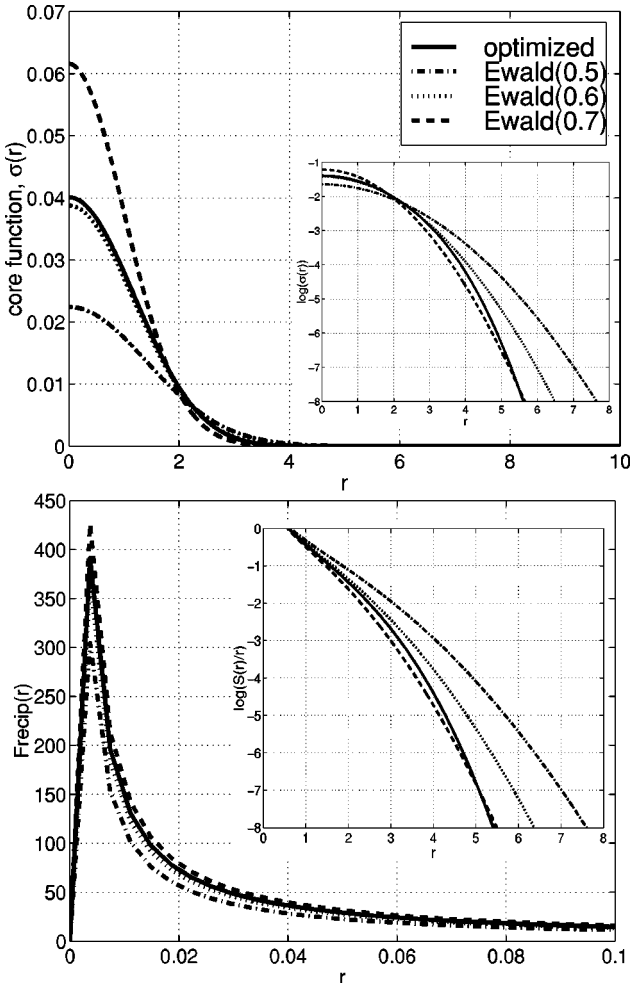


FIG. 6. Comparison of the core function, reciprocal force, and $S(r)/r$ function for the optimization of the rate of decay of the Fourier spectrum relative to $f(x;\alpha=1.7,\beta=0.98,n=13)$. (Top) the particle core function and its logarithm. (Bottom) the reciprocal force, along with $\log(S(r)/r)$. Comparison to the Ewald method ($\beta=0.5$, 0.6, and 0.7 solutions) is shown.

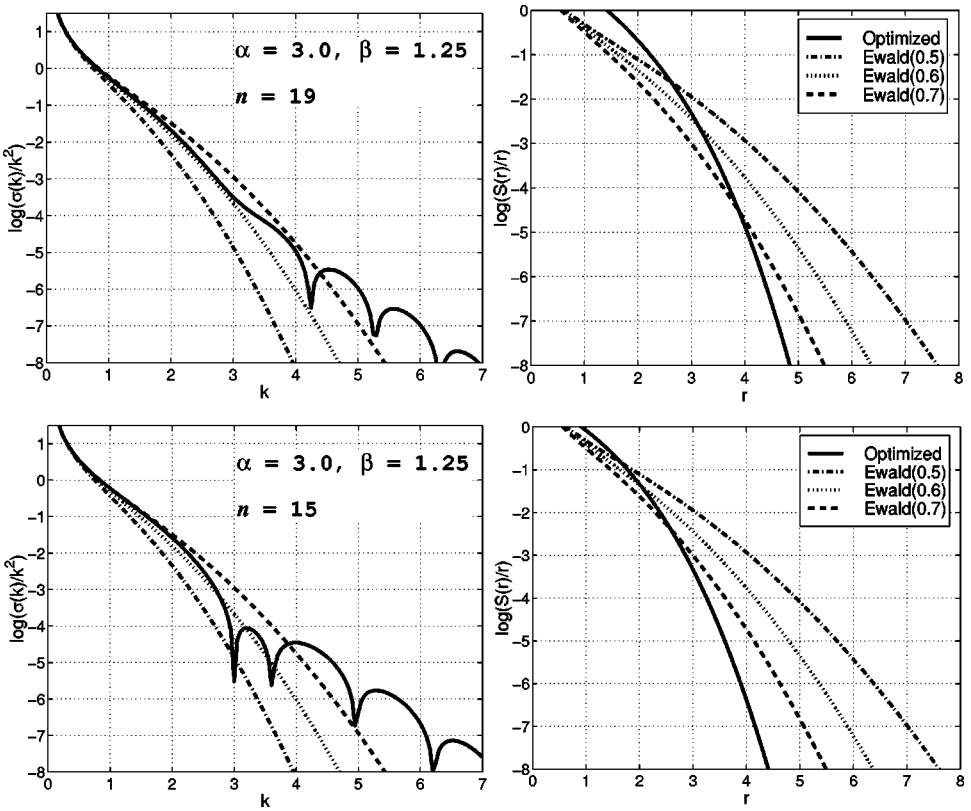


FIG. 7. Optimization of the rate of decay of the Fourier spectrum relative to $f(x;\alpha=3.0,\beta=1.25)$. A comparison of the Poisson kernel in reciprocal space and the logarithm of the $S(r)/r$ function is given relative to the Ewald $\beta=0.5$, 0.6, and 0.7 solutions. (Top) the solution for a 20-term expansion. (Bottom) solution for a 16-term expansion is shown.

was stated as an even polynomial of $r$ multiplied by the Ewald Gaussian function. All formulations incorporate the favorable decay rates of the Ewald method in the reciprocal and real space sums. For implementation into a particle-mesh algorithm, the formulation is not expected to introduce significant obstacles. The charge mesh assignment is typically done through a weighting function that is independent of the core function itself. Furthermore the core function, its Fourier transform, and the switch function can be tabulated or fit to a cubic spline for rapid evaluation if needed; alternatively, the use of defined recursion relations can be used for efficient calculation.

In general, faster decay rates in the real-space and reciprocal-space sums were shown relative to the Ewald method. The necessary background formulations were presented for rapid evaluation of the core and switch functions, and the core function's Fourier transform. Future directions of study will focus on incorporating the new lattice summations into a particle-mesh algorithm as well as the characterization of a time scale separation for the lattice.

## ACKNOWLEDGMENTS

The work is supported by NSF award ASC-9318159, NIH award R01 GM55164, and a John Simon Guggenheim fellowship.

## APPENDIX A: EVALUATION OF SWITCH FUNCTIONS

The introduction of the weighted Gaussian core functions, Eq. (25), requires the evaluation of Poisson's solution given by the integral representation of Eq. (18) in Sec. III. To this aim, the following definite and indefinite integrals are useful:

$$\int_0^r \exp(-\alpha^2 r^2)dr = \frac{\sqrt{\pi}}{2\alpha}\operatorname{erf}(\alpha r), \tag{A1}$$

$$\int_r^\infty \exp(-\alpha^2 r^2)dr = \frac{\sqrt{\pi}}{2\alpha}\operatorname{erfc}(\alpha r), \tag{A2}$$

$$\int r\exp(-\alpha^2 r^2)dr = -\frac{1}{2\alpha^2}\exp(-r^2\alpha^2)+C. \tag{A3}$$

The definite integrals

$$\int_r^\infty r^n \exp(-\alpha^2 r^2)dr, \quad n=3,5,\ldots, \tag{A4}$$

$$\int_0^r r^n \exp(-\alpha^2 r^2)dr, \quad n=2,4,\ldots \tag{A5}$$

are evaluated by factoring out $r^{n-1}$ from the integrand and integrating by parts once. With the results from the lower $n$ moments we can construct the hierarchy of integrals given as

$$\int_0^r r^{2n+2}\exp(-\alpha^2 r^2)dr = \frac{A_n^{-1}}{4\pi}\operatorname{erf}(\alpha r) - P_{2n+2}(r)\exp(-\alpha^2 r^2); \quad n=1,2,\ldots, \tag{A6}$$

$$\int_r^\infty r^{2n+1}\exp(-\alpha^2 r^2)dr$$

$$=P_{2n+1}(r)\exp(-\alpha^2 r^2);\quad n=1,2,\ldots, \tag{A7}$$

where $P_n(r)$ can be found from the recursion relation

$$P_0(r)=0,\quad P_1(r)=\frac{1}{2\alpha^2}, \tag{A8}$$

$$P_n(r)=\frac{r^{n-1}}{2\alpha^2}+\frac{n-1}{2\alpha^2}P_{n-2}(r). \tag{A9}$$

The normalizing constants are given by

$$A_0^{-1}=\frac{\pi^{3/2}}{\alpha^3}, \tag{A10}$$

$$A_n^{-1}=\frac{2n+1}{2\alpha^2}A_{n-1}^{-1}. \tag{A11}$$

Finally we have for the radially symmetric core function

$$\sigma_n(r)=A_n r^{2n}\exp(-\alpha^2 r^2);\quad n=0,1,2,\ldots, \tag{A12}$$

a switch function given by

$$S_n(r)=1-4\pi\int_0^r r^2\sigma_n(r)dr-4\pi r\int_r^\infty r\sigma_n(r)dr, \tag{A13}$$

$$S_0(r)=\mathrm{erfc}(r), \tag{A14}$$

$$S_n(r)=\mathrm{erfc}(r)+4\pi A_n(P_{2n+2}(r)-rP_{2n+1}(r))\times\exp(-\alpha^2 r^2);\quad n=1,2,\ldots. \tag{A15}$$

## APPENDIX B: EVALUATION OF THE DIRECT PAIRWISE INTERACTION

In Sec. IV A 2 we introduced a piecewise smooth core function that can be formulated to exactly satisfy the pairwise interaction splitting, namely the reciprocal potential and force component vanish for a particle separation less than a specified value $r_c$. The formulation requires the evaluation of the Fourier transform and radial symmetric solution to Poisson's equation for a core function of the form

$$\sigma(r;\beta,r_c,n)=\begin{cases}0 & r\leqslant r_c\\ (r-r_c)^{2n}\exp(-\beta^2(r-r_c)^2) & r>r_c\end{cases},\quad n=1,2,3,\ldots. \tag{B1}$$

The Fourier transform requires a closed form solution to

$$\int_{r_c}^\infty r(r-r_c)^{2n}\exp(-\beta^2(r-r_c)^2)\sin(kr)dr. \tag{B2}$$

With a change of variables $u=r-r_c$ we have

$$\int_0^\infty (u+r_c)u^{2n}\exp(-\beta^2u^2)\sin(k(u+r_c))du, \tag{B3}$$

and noting that $\sin(k(u+r_c))=\sin(ku)\cos(kr_c)+\cos(ku)\times\sin(kr_c)$ we are left with four integrals to evaluate. To this aim we use the following integrals,[37]

$$\int_0^\infty x^{\mu-1}\exp(-\beta x^2)\sin(\gamma x)dx$$

$$=\frac{\gamma\exp\left(-\frac{\gamma^2}{4\beta}\right)}{2\beta^{(\mu+1)/2}}\Gamma\left(\frac{1+\mu}{2}\right)\ {}_1F_1\left(1-\frac{\mu}{2};\frac{3}{2};\frac{\gamma^2}{4\beta}\right),$$

$$\int_0^\infty x^{\mu-1}\exp(-\beta x^2)\cos(\gamma x)dx$$

$$=\frac{\beta^{-\mu/2}}{2}\Gamma\left(\frac{\mu}{2}\right)\exp\left(-\frac{\gamma^2}{4\beta}\right)\ {}_1F_1\left(\frac{1}{2}-\frac{\mu}{2};\frac{1}{2};\frac{\gamma^2}{4\beta}\right),$$

$$\int_0^\infty x^{2n}\exp(-\beta^2x^2)\cos(\gamma x)dx$$

$$=\frac{(-1)^n\sqrt{\pi}}{(2\beta)^{2n+1}}\exp\left(-\frac{\gamma^2}{4\beta^2}\right)\mathrm{H}_{2n}\left(\frac{\gamma}{2\beta}\right),$$

$$\int_0^\infty x^{2n+1}\exp(-\beta^2x^2)\sin(\gamma x)dx$$

$$=\frac{(-1)^n\sqrt{\pi}}{(2\beta)^{2n+2}}\exp\left(-\frac{\gamma^2}{4\beta^2}\right)\mathrm{H}_{2n+1}\left(\frac{\gamma}{2\beta}\right).$$

We can therefore evaluate the following definite integrals as:

$$\int_0^\infty u^{2n+1}\exp(-\beta^2u^2)\sin(ku)du$$

$$=\frac{(-1)^n\sqrt{\pi}}{(2\beta)^{2n+2}}\exp\left(-\frac{k^2}{4\beta^2}\right)\mathrm{H}_{2n+1}\left(\frac{k}{2\beta}\right), \tag{B4}$$

$$\int_0^\infty u^{2n+1}\exp(-\beta^2u^2)\cos(ku)du$$

$$=\frac{\Gamma(n+1)}{2\beta^{n+1}}\exp\left(-\frac{k^2}{4\beta^2}\right)\ {}_1F_1\left(-\frac{2n+1}{2};\frac{1}{2};\frac{k^2}{4\beta^2}\right), \tag{B5}$$

$$\int_0^\infty u^{2n}\exp(-\beta^2u^2)\sin(ku)du$$

$$=\frac{k\Gamma(n+1)}{2\beta^{n+1}}\exp\left(-\frac{k^2}{4\beta^2}\right)\ {}_1F_1\left(\frac{1-2n}{2};\frac{3}{2};\frac{k^2}{4\beta^2}\right), \tag{B6}$$

$$\int_0^\infty u^{2n}\exp(-\beta^2u^2)\cos(ku)du$$

$$=\frac{(-1)^n\sqrt{\pi}}{(2\beta)^{2n+1}}\exp\left(-\frac{k^2}{4\beta^2}\right)\mathrm{H}_{2n}\left(\frac{k}{2\beta}\right). \tag{B7}$$

Noting that the confluent hypergeometric function ${}_1F_1(a;b;z)$ can be reduced to more familiar special functions,[41] namely,

$${}_1F_1\left(\frac{1}{2}-\frac{1}{2}n;\frac{3}{2};x^2\right)=2^{-n}\mathrm{H}_n(x)/x,$$

$${}_1F_1\left(-\frac{1}{2}n;\frac{1}{2};\frac{1}{2}x^2\right)=2^{-n/2}\exp(x^2/4)D_n(x).$$

Furthermore, the Weber function has the relation $\exp(x^2/4)D_n(x)=2^{-n/2}\mathrm{H}_n(x/\sqrt{2})$. These relations establish,

$$ {}_1F_1\left(\frac{1-2n}{2};\frac{3}{2};\frac{k^2}{4\beta^2}\right)=\frac{2\beta}{k}2^{-2n}\mathrm{H}_{2n}\left(\frac{k}{2\beta}\right), \tag{B8}$$

$$ {}_1F_1\left(-\frac{2n+1}{2};\frac{1}{2};\frac{k^2}{4\beta^2}\right)=\frac{1}{2^{2n+1}}\mathrm{H}_{2n+1}\left(\frac{k}{2\beta}\right). \tag{B9}$$

Evaluation of the cases for $n=1$ and 2 lead us directly to the result of Eq. (56) in Sec. IV A 2.

Next, we evaluate the solution to Poisson's equation, $\phi(r)$, where the core function is our piecewise smooth function Eq. (B1). An integral expression for the potential $\phi(r)$, for a spherically symmetric core function, was presented in Sec. II and is given here for the piecewise smooth case,

$$\phi(r)=\frac{4\pi}{r}\int_{r_c}^{r}d\xi(\xi^2)\sigma(\xi-r_c)+4\pi\int_{r}^{\infty}d\xi(\xi)\sigma(\xi-r_c). \tag{B10}$$

For the first term in Eq. (B10) we make the change of variables $v=\xi-r_c$ and $u=r-r_c$, and note that $(u+r_c)^2=u^2+2ur_c+r_c$. From the results of Appendix B we have,

$$\int_0^u v^{2n+2}\exp(-\beta^2v^2)dv = \frac{A_n^{-1}}{4\pi}\mathrm{erf}(\beta u)-P_{2n+2}(u)\exp(-\beta^2u^2);\quad n=1,2,3,\ldots, \tag{B11}$$

$$\int_0^u v^{2n}\exp(-\beta^2v^2)dv = \frac{A_{n-1}^{-1}}{4\pi}\mathrm{erf}(\beta u)-P_{2n}(u)\exp(-\beta^2u^2), \tag{B12}$$

and with the application of integration by parts we have

$$\int_0^u v^{2n+1}\exp(-\beta^2v^2)dv = -\frac{u^2}{2\beta^2}\exp(-\beta^2u^2)+\frac{2n}{2\beta^2}\int_0^u v^{2n-1}\exp(-\beta^2v^2)dv,$$

which leads directly to

$$\int_0^u v^3\exp(-\beta^2v^2)dv = \left(-\frac{u^2}{2\beta^2}-\frac{2}{(2\beta^2)^2}\right)\exp(-\beta^2u^2)+\frac{2}{(2\beta^2)^2}, \tag{B13}$$

$$\int_0^u v^5\exp(-\beta^2v^2)dv = \left(-\frac{u^4}{2\beta^2}-\frac{4u^2}{(2\beta^2)^2}-\frac{8}{(2\beta^2)^3}\right)\exp(-\beta^2u^2)+\frac{8}{(2\beta^2)^3}. \tag{B14}$$

With these results we are able to evaluate analytical expressions for the first term in Eq. (B10) with $n=1$ and 2. Lastly we evaluate the second term in the integral equation for $\phi(r)$ by setting $v=\xi-r_c$ and examine the definite integral,

$$\int_r^\infty \xi\sigma(\xi-r_c)d\xi=\int_{r-r_c}^\infty (v+r_c)v^{2n}\exp(-\beta^2v^2)dv.$$

To this aim the following integrals are readily established:

$$\int_{r-r_c}^\infty v^{2n+1}\exp(-\beta^2v^2)dv = P_{2n+1}(r-r_c)\exp(-\beta^2(r-r_c)^2), \tag{B15}$$

and by applying integration by parts and setting $u=r-r_c$ we have

$$\int_u^\infty v^{2n}\exp(-\beta^2v^2)dv=\frac{u^{2n-1}}{2\beta^2}\exp(-\beta^2u^2)+\frac{2n-1}{2\beta^2}\times\int_w^\infty v^{2n-2}\exp(-\beta^2v^2)dv$$

which leads directly to

$$\int_u^\infty v^2\exp(-\beta^2v^2)dv=\frac{u}{2\beta^2}\exp(-\beta^2u^2)+\frac{\sqrt{\pi}}{2\beta^2 2\beta}\mathrm{erfc}(\beta u), \tag{B16}$$

$$\int_u^\infty v^4\exp(-\beta^2v^2)dv=\left(\frac{u^3}{2\beta^2}+\frac{3u}{(2\beta^2)^2}\right)\exp(-\beta^2u^2)+\frac{3\sqrt{\pi}}{(2\beta^2)^2 2\beta}\mathrm{erfc}(\beta u). \tag{B17}$$

With the above results we arrive at the complete expression for the Poisson's solution given in Sec. IV A 2, Eqs. (49) and (50).

## APPENDIX C: POTENTIALS, TRANSFORMS, AND INTEGRAL COEFFICIENTS FOR A PAIRWISE INTERACTION CORE FUNCTION

Here we present the potentials and integral coefficients for a core function that results in a minimal departure from the tradition Ewald formulation, Eq. (58),

$$\sigma(r)=\begin{cases}0 & r\leqslant r_c\\ (a_1A_1(r_c)(r-r_c)+a_2A_2(r_c)(r-r_c)^2)\\ \quad\times\exp(-\beta^2(r-r_c)^2) & r>r_c.\end{cases}$$

An important check of the potential functions and resulting switch functions are that they satisfy the following continuity conditions:

$$\{\sigma(r),S(r),\phi(r)\}\in C^0,\quad \text{at } r=r_c, \tag{C1a}$$

$$\{S(r),\phi(r)\}\in C^1,\quad \text{at } r=r_c. \tag{C1b}$$

The detailed integral evaluations are easily derived from the results in Appendices A and B, and with integration by parts.

The optimization coefficients $a_1$ and $a_2$ are given by Eq. (45a) and Eq. (45b), and for the coefficients $C_1$ and $C_2$, see Eq. (44), we have

$$C_1=\frac{\sqrt{\pi}}{4\beta^3}+\frac{r_c}{2\beta^2}, \tag{C2a}$$

$$C_2=\frac{2}{(2\beta^2)^2}+\frac{r_c\sqrt{\pi}}{4\beta^3}. \tag{C2b}$$

For normalization coefficients $A_1(r_c)$ and $A_2(r_c)$ we have

$$A_1^{-1}(r_c)=\frac{1+r_c^2\beta^2}{2\beta^4}+\frac{r_c\sqrt{\pi}}{2\beta^3}, \tag{C3a}$$

$$A_2^{-1}(r_c)=\frac{\sqrt{\pi}}{4\beta^3}\left(r_c^2-\frac{3}{2\beta^2}\right)+\frac{r_c}{\beta^4}. \tag{C3b}$$

The potential functions associated with the $r-r_c$ and $(r-r_c)^2$ moments, after some algebraic manipulation, are, respectively, given as, $\phi(r;\beta,r_c,1)=\phi(r;\beta,r_c,2)=0$ for $r\leqslant r_c$, and for $r>r_c$ we have

$$\begin{aligned}\phi(r;\beta,r_c,1)=&\frac{1}{r}\left[\frac{r_c\sqrt{\pi}}{2\beta^3}\operatorname{erf}(\beta u)+\frac{1+r_c^2\beta^2}{2\beta^4}\right]\\&-\frac{\exp(-\beta^2u^2)}{r}\left[\frac{(u+r_c)^2}{2\beta^2}+\frac{1}{\beta^2}\right]\\&+\left(\frac{u}{2\beta^2}+\frac{r_c}{2\beta^2}\right)\exp(-\beta^2u^2)\\&+\frac{\sqrt{\pi}}{4\beta^3}\operatorname{erfc}(\beta u),\end{aligned} \tag{C4a}$$

$$\begin{aligned}\phi(r;\beta,r_c,2)=&\frac{1}{r}\left[\frac{\sqrt{\pi}}{4\beta^3}\left(r_c^2-\frac{3}{2\beta^2}\right)\operatorname{erf}(\beta u)+\frac{r_c}{\beta^4}\right]\\&-\frac{\exp(-\beta^2u^2)}{r}\left[\frac{3u-4r_c}{4\beta^4}-\frac{u(u+r_c)^2}{2\beta^2}\right]\\&+\frac{u^2+ur_c+2}{2\beta^2}\exp(-\beta^2u^2)\\&+\frac{r_c\sqrt{\pi}}{4\beta^3}\operatorname{erfc}(\beta u),\end{aligned} \tag{C4b}$$

where $u=r-r_c$ and the switch function is given by Eq. (54) in Sec. IV A 2.

Lastly, the Fourier transform of the core function is given by the sum of the transforms for the $r-r_c$ and $(r-r_c)^2$ moments,

$$\hat{\sigma}(k;\beta,r_c)=a_1A_1(r_c)\hat{\sigma}(k;\beta,r_c,1)+a_2A_2(r_c)\hat{\sigma}(k;\beta,r_c,2), \tag{C5}$$

which are, respectively, given as

$$\begin{aligned}\hat{\sigma}(k;\beta,r_c,1)=&\frac{4\pi}{k}\exp\left(-\frac{k^2}{4\beta^2}\right)\left[\cos(kr_c)\left(\frac{1}{2\beta}\mathrm{H}_2\left(\frac{k}{2\beta}\right)\right.\right.\\&\left.+\frac{r_c\sqrt{\pi}}{(2\beta)^2}\mathrm{H}_1\left(\frac{k}{2\beta}\right)\right)+\sin(kr_c)\\&\left.\times\left(\frac{r_c}{4\beta}\mathrm{H}_1\left(\frac{k}{2\beta}\right)-\frac{\sqrt{\pi}}{(2\beta)^3}\mathrm{H}_2\left(\frac{k}{2\beta}\right)\right)\right],\end{aligned} \tag{C6a}$$

$$\begin{aligned}\hat{\sigma}(k;\beta,r_c,2)=&\frac{4\pi}{k}\exp\left(-\frac{k^2}{4\beta^2}\right)\left[\cos(kr_c)\left(\frac{r_c}{4\beta}\mathrm{H}_2\left(\frac{k}{2\beta}\right)\right.\right.\\&\left.-\frac{\sqrt{\pi}}{(2\beta)^4}\mathrm{H}_3\left(\frac{k}{2\beta}\right)\right)+\sin(kr_c)\\&\left.\times\left(\frac{1}{16\beta^2}\mathrm{H}_3\left(\frac{k}{2\beta}\right)-\frac{r_c\sqrt{\pi}}{(2\beta)^3}\mathrm{H}_2\left(\frac{k}{2\beta}\right)\right)\right],\end{aligned} \tag{C6b}$$


[1] W. Jones and N. R. March, *Theoretical Solid State Physics* (Wiley, New York, 1973).
[2] M. P. Allen and D. J. Tildesley, *Computer Simulations of Liquids* (Oxford University Press, Oxford, 1989).
[3] F. Y. Haij, J. Chem. Phys. **70**, 4369 (1979).
[4] E. F. Bertaut, J. Chem. Phys. **39**, 97 (1978).
[5] D. M. Heyes, J. Chem. Phys. **74**, 1924 (1981).
[6] R. W. Hockney and J. W. Eastwood, *Computer Simulation Using Particles* (Institute of Physics, London, 1988).
[7] P. P. Ewald, Ann. Phys. (Leipzig) **64**, 253 (1921).
[8] J. Norberg and L. Nilsson, Biophys. J. **79**, 1537 (2000).
[9] A. P. Smith and N. W. Ashcroft, Phys. Rev. B **38**, 12942 (1988).
[10] R. D. Misra, Proc. Cambridge Philos. Soc. **36**, 173 (1940).
[11] M. Born and M. Bradburn, Proc. Cambridge Philos. Soc. **39**, 104 (1943).
[12] N. Karasawa and W. A. Goddard III, J. Phys. Chem. **93**, 7321 (1989).
[13] U. Essmann, L. Perera, M. L. Berkowitz, T. Darden, H. Lee, and L. G. Pedersen, J. Chem. Phys. **103**, 8577 (1995).
[14] G. Salin and J. M. Caillol, J. Chem. Phys. **113**, 10459 (2000).
[15] H. J. C. Berendson, in *Computer Simulation of Biomolecular Systems*, edited by W. F. van Gunsteren, P. K. Weiner, and A. J. Wilkinson (ES-COM, The Netherlands, 1993), Vol. 2, p. 161.
[16] T. Darden, D. York, and L. Pedersen, J. Chem. Phys. **98**, 10089 (1993).
[17] T. Darden, L. Perera, L. Leping, and L. Pedersen, Structure (London) **7**, R55 (1999).
[18] D. York and W. Yang, J. Chem. Phys. **101**, 3298 (1994).
[19] M. Deserno and C. Holm, J. Chem. Phys. **109**, 7678 (1998).
[20] L. Greengard and V. Rokhlin, Acta Numerica **6**, 2298 (1998).
[21] H. G. Peterson, D. Soelvason, J. W. Perram, and E. R. Smith, J. Chem. Phys. **101**, 8870 (1994).
[22] B. A. Luty, I. G. Tironi, and W. F. van Gunsteren, J. Chem. Phys. **103**, 3014 (1995).
[23] M. Kawata and M. Mikami, J. Comput. Chem. **21**, 201 (2000).
[24] Z. H. Duan and R. Krasny, J. Chem. Phys. **113**, 3492 (2000).
[25] P. F. Batcho, D. A. Case, and T. Schlick, J. Chem. Phys. **115**, 4003 (2001).
[26] T. Schlick, Structure (London) **9**, R45 (2001).
[27] P. M. Morse and H. Feshbach, *Methods of Theoretical Physics* (McGraw–Hill, New York, 1953), Vol. 2.
[28] C. Kittel, *Introduction to Solid State Physics* (Wiley, New York, 1976).
[29] D. J. Adams and G. S. Dubey, J. Comput. Phys. **72**, 156 (1987).
[30] S. W. de Leeuw, J. W. Perram, and E. R. Smith, Proc. R. Soc. London, Ser. A **373**, 27 (1980).
[31] A. Grzybowski, E. Gwozdz, and A. Brodka, Phys. Rev. B **61**, 6706 (2000).
[32] E. L. Pollock and J. Glosili, Comput. Phys. Commun. **95**, 95 (1996).
[33] P. F. Batcho, Phys. Rev. E **61**, 7169 (2000).
[34] P. F. Batcho, Phys. Rev. A **57**, 4246 (1998).
[35] D. Gottlieb and S. A. Orszag, *Numerical Analysis of Spectral Methods:*

*Theory and Applications* (SIAM, Philadelphia, 1977).
[36] P. H. Hunenberger, J. Chem. Phys. **113**, 10464 (2000).
[37] I. S. Gradshteyn and I. M. Ryzhik, *Table of Integrals, Series, and Products*, 5th ed. (Academic, San Diego, 1994).
[38] M. Zhang and R. D. Skeel, Appl. Numer. Math. **25**, 297 (1997).
[39] A. Cheng and K. M. Merz, Jr., J. Phys. Chem. B **103**, 5396 (1999).
[40] P. Procacci, M. Marchi, and G. J. Martyna, J. Chem. Phys. **108**, 8799 (1998).
[41] M. Abramowitz and I. A. Stegun, *Handbook of Mathematical Functions* (Dover, New York, 1965).